Ann. Rev. Astron. Astrophys. 1982. 20:163-90

INTERSTELLAR MOLECULAR HYDROGEN

J. Michael Shull

Joint Institute for Laboratory Astrophysics and Laboratory for Atmospheric and Space Physics, University of Colorado, Boulder, Colorado 80309

Steven Beckwith

Department of Astronomy, Cornell University, Ithaca, New York 14853

1. INTRODUCTION

After atomic hydrogen, helium, and their ions, the Universe probably contains more mass in molecular hydrogen (H_2) than in any other species. In our Galaxy, the molecules reside primarily in the vast complexes of molecular clouds that contain 10–20% of the mass in the inner disk. In a continuous exchange of matter, the stars supply matter to the interstellar medium through winds and explosions, and the gas coalesces into clouds, which collapse to form new stars. The state of the clouds and the rate at which they evolve depend on heating and cooling of matter composed almost entirely of H_2.

Eddington (1937), Strömgren (1939), and Gold (1961) suggested that H_2 might exist in portions of interstellar space. Detailed studies by Gould & Salpeter (1963) and Hollenbach et al. (1971) predicted large fractional abundances of H_2 in interstellar clouds. However, the hydrogen molecule remained unobserved in the interstellar medium until Carruthers (1970) detected its electronic absorption spectrum toward the star ξ Persei with a rocket-borne ultraviolet (uv) spectrometer. Observations of the electronic lines increased rapidly with the launch of the *Copernicus* satellite in 1972 (Rogerson et al. 1973). The uv absorption studies are limited to relatively unreddened clouds, however, and cannot probe the dense clouds seen in CO radio emission (Wilson et al. 1970). Gautier et al. (1976) and Treffers et al. (1976) discovered H_2 emission lines from the $v=1\text{-}0$ vibration-rotation band in infrared (IR)

0066-4146/82/0915-0163$02.00

spectra of the Orion molecular cloud and NGC 7027, a planetary nebula. An increasing number of objects are observed to emit vibration-rotation lines of H_2, but unfortunately the observations are limited to small quantities of gas. The fact that most hydrogen molecules in massive interstellar clouds remain hidden from our view is a continuing incentive to observers who wish to observe hydrogen directly.

Emission from H_2 is theoretically one of the principal means by which the interstellar gas cools under a variety of circumstances. Clouds can form stars only if the gravitational energy released by the collapse is radiated away before it heats the cloud. Peebles & Dicke (1967) and Saslaw & Zipoy (1967) pointed out that the cooling of primordial clouds with zero metal abundance would be dominated by small amounts of H_2, formed in gas-phase reactions as the cloud collapsed. Molecular hydrogen emission may also provide the primary coolant for interstellar shock waves (Field et al. 1968, Aannestad 1973a,b), produced when molecular clouds collide, or when stellar winds, H II regions, and supernovae encounter these clouds. The latter processes may be responsible for triggering bursts of star formation when the compressed gas behind the shock waves collapses (Elmegreen & Lada 1977, Gerola & Seiden 1978). The last decade has produced many studies of the role of molecular hydrogen in interstellar gas dynamics. At the same time, the quantum properties of the molecule, such as spontaneous transition rates and collision cross sections, were measured or calculated with increasing accuracy. At the time of the last review in these volumes (Field et al. 1966), H_2 had been detected only in planets and the atmospheres of some stars. In this article, we review some of the recent progress made on H_2 in the interstellar medium.

2. THE HYDROGEN MOLECULE

2.1 *Properties of the Hydrogen Molecule*

Herzberg (1950) describes the quantum mechanics of homonuclear molecules in some detail, and Field et al. (1966) summarize the notation for H_2. The ground-electronic state is denoted $X\,^1\Sigma_g^+$, and excited states are labeled alphabetically. The symbols (Σ, Π, Δ) denote the total electron angular momentum (0, 1, 2 in units $\hbar$), projected on the internuclear axis, k. Figure 1 shows the total energy as a function of internuclear separation for several of the electronic states. The electronic states are split by vibration and rotation of the nuclei. For electronic states with nonzero electronic angular momentum or spin (e.g. $^1\Pi_u$ or $^3\Sigma_g^+$), the nuclear rotation (R) combines with the electronic angular momentum (Λk) to form a resultant N, which then combines with the total electron spin S to form the total angular momentum vector J (Hund's case *b*). Nuclear spin is treated separately, as discussed below. For the ground electronic state, R and J are identical. Rotational levels are normally denoted by N and are assumed to be split into three components if S is 1.

The energy of each state is written (Herzberg 1950, Huber & Herzberg 1979) as an expansion in the quantum numbers (called a term value):

$$T(v,N) = T_e + \omega_e(v + \tfrac{1}{2}) - \omega_e x_e(v + \tfrac{1}{2})^2 + \omega_e y_e(v + \tfrac{1}{2})^3 + \dots \\ + B_v N(N + 1) - D_v N^2(N + 1)^2 + H_v N^3(N + 1)^3 + \dots .$$

T_e is the electronic energy corresponding to the minima in the potential curves. B_v, D_v, etc., are further expanded as power series in $(v + \frac{1}{2})$. The constants of the expansion are determined empirically from spectra of the molecule and are usually given in cm^{-1} (Fink et al. 1965, Beck et al. 1979). Use of the formula for very large v or N can lead to errors; some authors prefer to calculate $T(v,N)$

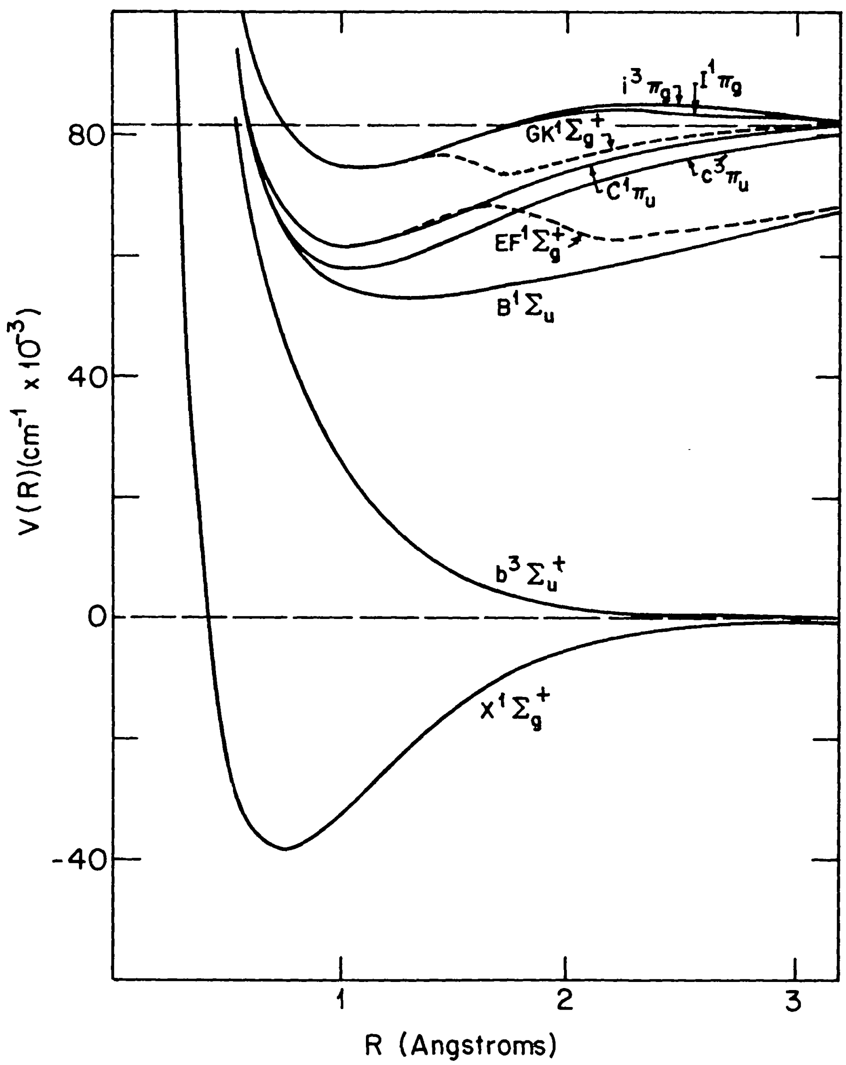

Figure 1 Total energy as a function of internuclear separation for low-lying states of H_2. Horizontal dashed lines denote total energy of two H atoms at infinite separation (both atoms in ground state; one atom in ground state and the other in the first excited states).

from potential curves (Black & Dalgarno 1976). Because many lines with large v or N have been observed in celestial sources, more accurate constants would be useful (see Jennings & Brault 1982).

The statistical weight of each level is a function of the rotational quantum number and the nuclear spin. Since the two nuclei are identical fermions, only one combination of nuclear spins is possible for each rotational level within an electronic state to preserve the antisymmetry of the overall wavefunction with respect to exchange of the nucleons. In the ground-electronic state, all the levels with odd J (identical to N in this case) are nuclear triplet states (ortho-hydrogen), and all the even J are singlet states (para-hydrogen). The statistical weight of a level J in the ground state is $3\,(2J + 1)$ for odd J and $(2J + 1)$ for even J.

Field et al. (1966) summarize the selection rules for electronic dipole transitions. Briefly, the projection of the electronic angular momentum changes by 0 or ± 1, the electronic spin does not change, states with subscript g combine only with states with subscript u and vice versa, and Σ states with + or − superscripts combine only with like Σ states. The vibrational quantum number changes according to the Franck-Condon principle. The first transitions from the electronic-ground state to the $B\,^1\Sigma_u^+$ and $C\,^1\Pi_u$ states are known as the Lyman and Werner bands, with energies from 11 to 14 eV. Morton & Dinerstein (1976) list the wavelengths and oscillator strengths for 420 lines in these bands.

Electric and magnetic dipole transitions between levels of different v and J within the ground-electronic state are forbidden, but electric quadrupole transitions may occur. The selection rules are $\Delta J = 0, \pm 2$, with 0-0 transitions forbidden. There is no strict selection rule on Δv owing to anharmonicity in the electronic potential functions. Transitions are labeled as $(v'\text{-}v'')\ O(J'')$, $Q(J'')$ and $S(J'')$ for $(J''\text{-}J') = 2, 0,$ or -2 ($'$ and $''$ superscripts refer to the upper and lower levels, respectively). Transitions with $\Delta v = \pm 1$ have energies ~0.5 eV and occur near 2 μm. The (0-0) rotational lines lie between 3 and 28 μm. Because H_2 has a very small moment of inertia, the rotational lines are widely spaced and easily separated by low-resolution spectrometers.

Turner et al. (1977) calculated the transition rates for the vibration-rotation transitions in the ground-electronic state. Although there are several discrepancies with experimentally derived rates (Scoville et al. 1982), the calculated values should be accurate to 10%, and the ratios to better than a few percent (Dalgarno, personal communication).

2.2 *Collisional Excitation and Dissociation Rates*

Nearly all theoretical calculations concerning H_2 emission and absorption lines require rate coefficients for excitation, de-excitation, or dissociation of H_2 by collisions with H_2 or H^0. In some high temperature regions, $H_2{-}e^-$ collisions are important in determining H_2 dissociation rates. In this section, we discuss the best available cross sections, provide convenient analytic fits to rate coefficients (Table 1), and outline the areas in need of further work.

The calculations of H-H_2 rotational excitation evolved from the rigid-rotator distorted-wave calculations of Nishimura (1968) to the close-coupling calculations of Chu & Dalgarno (1975) and McGuire & Krüger (1975) that suggest rates two to five times smaller than Nishimura's. Green & Truhlar (1979) find rates 20 to 40 times smaller; these are probably far too small. Schatz & Kuppermann (1976) discuss $J = 0 \rightarrow 1$ and $J = 0 \rightarrow 2$ excitation by reactive and non-reactive scattering. We feel the most conservative estimates of H-H_2 rotational excitation rates are those of Elitzur & Watson (1978) based on the "surprisal analysis" (Levine et al. 1976), or those of Shull & Hollenbach (1978) based on fits to theoretical cross sections. The latter rates agree with the Elitzur & Watson rates to better than 50% ($T > 500$ K), and are two to four times smaller than Nishimura's. None of these rates are known to a factor of ~5. Further work on H-H_2 rotational excitation is obviously needed, particularly at low energies ($T \cong 100$ K) and for $J \leq 5$.

Zarur & Rabitz (1974) and Green (1975) suggest that H_2-H_2 rotational excitation cross sections are comparable to those of H-H_2. More elaborate theoretical calculations, including analytic fits, may be found in Green et al. (1978).

H_2 vibrational excitation rates are more uncertain. Experimental data for H_2 ($v = 1 \rightarrow 0$) relaxation have been obtained by Audibert et al. (1974) for $40 < T < 500$ K and inferred from Ar-H_2 by Kieffer & Lutz (1966) and Dove & Teitelbaum (1974) for $1100 < T < 2700$ K. The analytic fits in Table 1 to the H_2-H_2 vibrational de-excitation rates from states (vJ), when summed over all possible downward transitions from $v = 1 \rightarrow 0$, yield close agreement with the experimental rates. Vibrational de-excitation rates drop off rapidly once the precollision translational kinetic energy becomes smaller than the

Table 1 H_2 collisional de-excitation rate coefficients

Collision type[b]	Rate coefficient ($cm^3\ s^{-1}$)[a]
A. *Rotational* (H^0-H_2 *or* H_2-H_2)	$\sigma_0 \bar{v}[1 - 1/b][1 + 1/b + E_T/kT]$
B. *Vibrational* (H^0-H_2)[c]	$(1.40 \times 10^{-13})\exp[(T/125) - (T/577)^2]; T < 1635$ K
	$(1.0 \times 10^{-12})T^{1/2}\exp[-1000/T]; T > 1635$ K
C. *Vibrational* (H_2-H_2)	$\sigma_0\bar{v}\exp[-4.2E_T/k(T + 1190)]$

[a]Rate coefficients for de-excitation from (vJ) to ($v'J'$) ($\Delta J = -2, 0, +2$ only); excitation rates follow from detailed balance. Parameters $\sigma_0 \cong 10^{-16}$ cm^2, $\bar{v} = (8kT/\pi\mu)^{1/2}$ with $\mu = m_H$ (H_2-H_2) or 0.67 m_H (H^0-H_2); $b = 1 + 0.1\ kT/E_T$; $E_T = E_{vJ} - E_{v'J'}$.

[b]References: A. Shull & Hollenbach (1978); B. Chu (1977, unpublished); C. Hollenbach (1981, personal communication).

[c]These rates are highly uncertain; Kwan (1977) uses unpublished reactive scattering rates of Schatz (1976), which are 50 to 100 times smaller.

"energy gap," $|E_{vJ} - E_{v'J'}|$. The work of Zarur & Rabitz (1974) suggests the approximate selection rule $\Delta J = 0, \pm 2$ ($J = 0 \rightarrow 0$ is allowed due to s-wave scattering).

Rate coefficients for H-H_2 vibrational excitation are dominated by reactive scattering:

$$H_A + H_B H_C(vJ) \rightarrow H_A H_B(v'J') + H_C.$$

Because of the exchange nature of the collision, ortho-para conversion and sizable rates in channels $\Delta J = 0, \pm 1, \ldots, \pm 5$ may result. The rates in Table 1 are based on fits to calculations of Chu (1977, unpublished) and Schatz (1976), quoted by Kwan (1977). There are significant uncertainties in these rates. (Chu's are much larger than Schatz's.)

Chu has also shown that H_2-H_2 vibrational excitation is complicated by "resonant rates" for collisions,

$$H_2(v_1 J_1) + H_2(v_2 J_2) \rightarrow H_2(v_3 J_3) + H_2(v_4 J_4),$$

in which the "energy defect," $\delta = |(E_3 + E_4 - E_1 - E_2)| \ll kT$. Such collisions may be important in depopulating H_2 excited vibrationally by uv radiation (Shull 1978a). Unfortunately, reliable rate coefficients do not exist.

Rates to levels $v > 1$ are highly uncertain, although the energy gap formalism suggests that $\Delta v = \pm 1$ transitions dominate. Although one could simply adopt the rates in Table 1 as a general formula for all v,J, Dalgarno & Roberge (1979) use the SSH formalism (Schwartz et al. 1952, Keck & Carrier 1965), in which rates for higher vibrational levels are related to $v = 1 \rightarrow 0$ rates by a multiplicative factor that increases with v. Dalgarno & Roberge (1979) point out that the magnitude of these high-v excitation rates is crucial in determining the rate of H_2 collisional dissociation at low density (see Section 3). Gerhart (1975), Douthat (1979), and Hollenbach & McKee (1980) describe e^--H_2 collision data. The first two papers are discussed further in section 5.2. The latter work shows that electronic collisions which spin-flip the H_2 from the bound $X\ ^1\Sigma_g^+$ state to the repulsive $b\ ^3\Sigma_u^+$ state at 8.8 eV are an important dissociating mechanism of H_2 behind low-density 50 km s^{-1} shocks. Collisions of H_2 with protons are discussed by Dalgarno et al. (1973) and Gentry & Giese (1975). At low temperatures, proton collisions provide the dominant mechanism of ortho-para ($J = 0 \leftrightarrow 1$) conversion.

3. CHEMICAL AND ENERGY BALANCE OF H_2

3.1 *Formation of Molecular Hydrogen*

Almost all of the H_2 produced in interstellar clouds probably forms on grain surfaces (Hollenbach & Salpeter 1970, 1971, Goodman 1978, Smoluchowski 1981, Watson 1976). The formation rate depends on the collision rate between

H atoms and grains, the probability that atoms are adsorbed on the grain surface (sticking probability), the mobility and lifetime of the atoms on the grain surface, and the probability that a molecule is ejected after formation. The formation rate (formations cm^{-3} s^{-1}) is usually written as $Rnn(\text{H I})$, where n and $n(\text{H I})$ are densities of total hydrogen and H I, respectively, and where $R(cm^3\ s^{-1})$ is a rate coefficient.

Molecule formation proceeds rapidly for grain temperatures less than a critical value, T_{cr}, between 20 K and 100 K; above this value, atoms evaporate from the grain surface before forming H_2 (Hollenbach & Salpeter 1971, Burke & Hollenbach 1980). For a Maxwellian velocity distribution of H atoms, the formation rate coefficient is approximately

$$R = (3 \times 10^{-17}\ \text{cm}^3\ \text{s}^{-1}) \frac{T_2^{1/2} f_a}{[1 + 0.4\,(T_2 + T_{g2})^{1/2} + 0.2\,T_2 + 0.08\,T_2^2]},$$

where T_2 and T_{g2} are atom and grain temperatures in units of 100 K, and f_a is the fraction of atoms which enter grain-binding sites before evaporating (Burke & Hollenbach 1980, Hollenbach & McKee 1979). This coefficient f_a is consistent with the sticking of all atoms with $V < 2$ km s^{-1}; gas-grain drift will modify this formula. Since the composition and structure of grain surfaces are highly uncertain, it is difficult to calculate the exact value of R. *Copernicus* uv data suggest that $R \approx (1\text{–}3) \times 10^{-17}$ cm^3 s^{-1} (Jura 1974).

Gas phase reactions are the only source of H_2 when grains are not present. The formation of H_2 during cloud collapse in the early Universe is thought to have proceeded through the following reactions (Yoneyama 1972, Hutchins 1976, and references therein):

$$H^0 + e^- \rightarrow H^- + h\nu$$
$$H^- + H^0 \rightarrow H_2 + e^-$$

The first reaction has been studied by Dalgarno & Kingston (1963), the second by Bieniek & Dalgarno (1979). Other reactions may form H_2 in the gas phase (Black 1978), but their rates are much slower in low-temperature, low-density regions. The above H^- reaction may also play a dominant role in the formation of H_2 in the interfaces between ionized and neutral gas (Black 1978).

Hydrogen molecules are destroyed by radiative and collisional dissociation. Direct radiative dissociation is unlikely, since the only dissociative transition stimulated by radiation longward of 912 Å is $X^1\Sigma_g^+ \rightarrow b^3\Sigma_u^+$, which is forbidden by the change in spin multiplicity. Most radiative dissociation proceeds in two steps (Stecher & Williams 1967): a transition from the ground state to the $B^1\Sigma_u^+$ or $C\ ^1\Pi_u$ (Lyman & Werner bands), followed ~11% of the time by a spontaneous decay to the vibrational continuum of the ground electronic state. In intense radiation fields, vibration-rotational levels may be excited, with correspondingly different dissociation rates. The original calculations have been modified for different situations by Dalgarno & Stephens (1970), Black & Dalgarno (1976), Shull (1978a), and London (1978).

Collisions with H or H_2 will normally dissociate H_2 when $T \geq 4000$ K (Kwan 1977, Hutchins 1976), although the rate is highly density-sensitive (Dalgarno & Roberge 1979). In dense clouds, the temperatures are too low to give appreciable collisional dissociation. Self-shielding in the Lyman and Werner bands (Hollenbach et al. 1971) and dust absorption will prevent uv radiation from penetrating far into the clouds. Thus, the cloud interiors are molecular, while the cloud surfaces are mostly atomic (Federman et al. 1979). Ionization of H_2 by cosmic rays and X rays can produce some heating of cloud interiors (Glassgold & Langer 1973), but it will not destroy a significant fraction of H_2. Collisional dissociation of H_2 occurs in shock fronts (Kwan 1977) and during the final stage of cloud collapse in star formation. The destruction of H_2 is also quite important in the collapse of primordial clouds, since H_2 is the primary coolant. The Jeans mass for the cloud fragments at the time of H_2 dissociation sets a lower limit on the mass of stars that will form.

3.2 *Cooling and Heating by H_2*

Molecular hydrogen can play a significant role in the thermal balance of interstellar clouds—both in cool (~100 K) diffuse clouds and in shocked molecular clouds (~2000 K). The H_2 radiative cooling function has recently been computed by Lepp & McCray (1982; see Figure 2), using the cross sections in Table 1. The cooling rate is density-dependent, owing to collisional de-excitation of excited levels. Because the radiative decay rates increase steeply with J, the critical density for de-excitation ranges from $n_{cr} \cong 10$ cm^{-3} for ($J = 2 \rightarrow 0$) to 10^{4-5} cm^{-3} for $J \gtrsim 7$ and most vibrational lines. For $n \gtrsim 10^6$ cm^{-3} (10^7 cm^{-3} for pure H_2), most rotational and vibrational levels are populated in near-thermal equilibrium, and the volume cooling rate (erg cm^{-3} s^{-1}) is proportional to n, rather than to n^2.

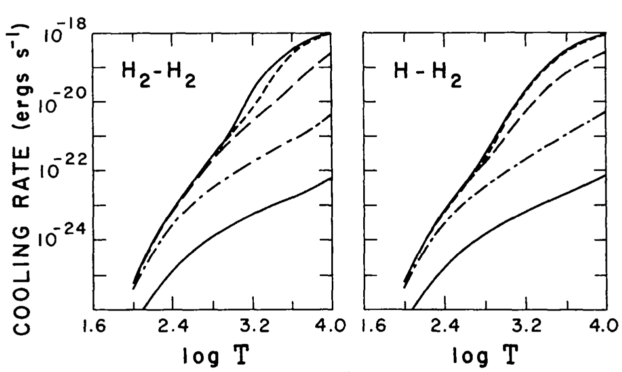

Figure 2 H_2 cooling rate, $L(T)/n$ (Lepp & McCray 1982), based on H_2-H_2 and H^0-H_2 collision rates in Table 1. For H^0-H_2 rates, $n(H_2) = 10^{-3}\,n(H^0)$. The five curves in each graph correspond to total H densities of 10^8, 10^6, 10^4, 10^2, and 10^0 cm^{-3} (top to bottom). Cooling rate is in thermal equilibrium ($L(T) \sim n$) for $n \geq 10^8$ cm^{-3}.

Dissociative cooling is also sensitive to density. Since dissociation is dominated by collisions from high vibrational levels, radiative decay results in a low-density ($n \leqslant 10^6$ cm^{-3}) dissociation rate orders of magnitude less than the experimental (thermal equilibrium) values (Breshears & Bird 1973). Dalgarno & Roberge (1979) present a model for an extreme case of these effects, in which dissociation is assumed to proceed solely from $v = 14$.

The heating produced by H_2 depends on the density, temperature, molecular fraction, ionization fraction, and uv/X-ray radiation field. Cosmic rays heat the cloud through the deposition of energy by the H_2^+ and secondary electrons produced by ionization (Glassgold & Langer 1973, Douthat 1979). This heat deposition is more efficient than in atomic hydrogen, owing primarily to dissociative encounters of H_2^+ with H_2 or electrons. Collisional de-excitation of levels excited by uv absorption may transfer energy from the radiation field to the gas. Finally, if a sizable fraction (say 10–30%) of the 4.48 eV H_2 binding energy can be released in the form of translational kinetic energy, H_2 formation heating may be an important heat source in diffuse clouds (Jura 1976) or in dissociation fronts driven by the uv radiation from O stars (London 1978). The importance of formation heating for diffuse clouds is quite dependent on the total surface area in small (50 Å) grains and to the fraction of the 4.48 eV that goes into the translational energy of a molecule as it leaves the grain (Black & Dalgarno 1976, Hunter & Watson 1978).

4. OBSERVATIONS

4.1 *Ultraviolet Studies*

Although H_2 absorption studies have not penetrated the giant molecular clouds, uv spectroscopic studies of H_2 by *Copernicus* have furnished information about physical conditions in diffuse interstellar clouds (Spitzer & Jenkins 1975). A curve-of-growth analysis of absorption lines in the H_2 Lyman bands ($\lambda < 1120$Å) and the Werner bands ($\lambda < 1021$ Å) provides column densities, $N(J)$, in rotational states J of the ground vibrational and electronic state. The total column density, $N(H_2)$, as well as the distribution over rotational levels, may be used to study the formation-destruction equilibrium of H_2, the kinetic temperature of the cloud, the hydrogen particle density, and the uv radiation field (Jura 1974, 1975a,b). In several instances, multiple absorption components at different velocities have been studied (Spitzer & Morton 1976, Shull & York 1977). The uv observations and diagnostic models have also been discussed in previous reviews (Spitzer & Jenkins 1975, Spitzer 1976).

The strongest uv absorption lines of H_2 arise from the $J = 0$ and 1 levels: the $R(0)$, $R(1)$, and $P(1)$ Lyman lines and the $R(0)$, $R(1)$, and $Q(1)$ Werner lines (Spitzer et al. 1974). The relative populations of $J = 0$ and 1 are established primarily by thermal proton collisions, since line self-shielding reduces the effects of uv-pumping dramatically in saturated lines. Therefore, the ratio of column densities is given by

$$\frac{N(1)}{N(0)} = \frac{g_1}{g_0} \exp\left(-E_{01}/kT_{01}\right) = 9 \exp\left(-170 \text{ K}/T_{01}\right), \tag{1}$$

where g_0 and g_1 are statistical weights of $J = 0$ and 1, respectively. In 13 stars with saturated $R(0)$ and $R(1)$ lines, Spitzer & Cochran (1973) found a mean cloud kinetic temperature $\langle T_{01} \rangle = (81 \pm 13)$ K, in general agreement with the mean value of 60–80 K found from comparing 21-cm absorption and emission (Hughes et al. 1971, Radhakrishnan et al. 1972). A more extensive survey of *Copernicus* data (Savage et al. 1977) found $\langle T_{01} \rangle = (77 \pm 17)$ K, with a range from 45 to 128 K. These temperatures are key observational constraints on heating sources of diffuse interstellar clouds—still a controversial problem.

The populations of higher-J levels are determined by collisions, uv- and formation-pumping [rotational and vibrational excitation following H_2 formation on grains], and radiative cascade (Spitzer & Zweibel 1974). The observed column densities in levels with $J > 2$ are fitted by excitation temperatures, T_{ex}, ranging from 300 to 1100 K (Spitzer & Cochran 1973). This range reflects either variations in the uv radiation field (Jura 1975a,b) or a range of shock velocities (Aannestad & Field 1973, Elitzur & Watson 1980).

Detailed models of the rotational populations of H_2 have been made by Jura (1975a,b), Black & Dalgarno (1977), Black et al. (1978), and Federman & Glassgold (1980). The column densities in high rotational levels ($J = 4,5$) are fixed by the rate of uv-pumping and formation-pumping. The intermediate rotational levels ($J = 2,3$) have longer radiative lifetimes, and may be deexcited by collisions. Therefore, the ratios $N(5)/N(1)$ and $N(4)/N(0)$ serve as measures of the uv radiation field, while $N(3)/N(1)$ and $N(2)/N(0)$ determine the collision rate (and hence the density n). The ratio of the total $N(H_2)$ to N(H I) determines the H_2 formation rate coefficient, R, once n is known. The H_2 column densities, together with column densities of trace molecules, also provide observational checks on multi-temperature-component models of diffuse clouds (Black & Dalgarno 1977, Snow 1977).

In studies of 16 lines of sight, Jura (1975a,b) found that R lies between $(1\text{–}3) \times 10^{-17}$ cm^3 s^{-1}, that n ranges from 10 to 1000 cm^{-3}, and that at least half the clouds are illuminated by uv radiation fields 5 to 30 times stronger than the mean interstellar field at 1000 Å (Jura 1974). These large inferred uv intensities suggest that the H_2 clouds lie within 10–30 pc of the OB stars used as background sources. The gas pressure, nT, for these clouds far exceeds the characteristic interstellar value $\sim 10^3$ cm^{-3} K, implying a connection between the H_2 clouds and OB stars (Spitzer & Jenkins 1975). Models of H_2 rotational excitation in circumstellar shells driven by OB-star winds have been described by Hollenbach et al. (1976).

Evidently, rotationally excited H_2 may be produced by shocks or by uv-pumping. The shock models may have difficulties explaining the data toward several stars with weak $R(0)$ and $R(1)$ lines (e.g. ζ Pup and τ Sco), for which a large rotational temperature fits all observed column densities down to $J = 0$. However, evidence in other instances suggests that the H_2 is associated with supersonic shells. For example, Frisch & Jura (1980) have found a correlation between the rotational excitation of H_2 and the column density of CH^+ (CH^+ is currently believed to form in hot postshock gas.) Further studies of CH^+ and H_2 toward stars in the Perseus OB2 association and the Pleiades (Federman 1980, 1982) suggest that shocks may play a role in H_2 rotational excitation, particularly in late B stars.

The largest base of *Copernicus* H_2 data is the survey of $J = 0,1$ column densities by Savage et al. (1977). Their survey confirms the earlier result of Spitzer & Jenkins (1975) that the molecular fraction, $f = 2N(H_2)/[N(\text{H I}) + 2N(H_2)]$, is correlated with $E(\text{B-V})$ and $N(\text{H I} + 2H_2)$. They find that f undergoes a transition from low values (<0.01) to high values (>0.01) when $E(\text{B-V}) \approx 0.08$ (Figure 3), which presumably reflects the self-shielding of H_2 (Federman et al. 1979). Corrected for sampling biases, the *Copernicus* survey provides the following line-of-sight averages for H_2 in diffuse clouds within distances $D < 500$ pc of the Sun: $\langle n(H_2)\rangle = 0.14\ \text{cm}^{-3}$, $\langle n(\text{H I})\rangle = 0.86\ \text{cm}^{-3}$, and $\langle f\rangle = 0.25$. For stars with saturated $J = 0,1$ lines, T_{01} shows a slight correlation with $\langle n(\text{H})\rangle$ (Figure 3). While $\langle n(\text{H})\rangle \equiv N(\text{H I} + 2H_2)/D$ is only a crude estimate of the physical density of the H_2 clouds, the correlation in Figure 3 implies that T_{01} may be lower in denser clouds, consistent with current ideas of cloud heating and cooling.

Ultraviolet observations of H_2 are not limited to interstellar clouds. Recently, approximately 100 emission lines between 1170 and 1700 Å in high-resolution sunspot spectra were identified as belonging to the H_2 Lyman bands (Jordan et al. 1978). The observed lines originate from only a few levels in the upper electronic state, pumped from the $v = 2$ vibrational level by resonance fluorescence with Lα. Shull (1978b) made a theoretical study of this process and pointed out several other resonances of H_2 Lyman and Werner bands with Lβ, N II λ1084, N II λ989, O VI λ1032, and C II λ1036. Resonance fluorescence with interstellar H_2 is probably limited to shocked clouds near sources of Lα (planetary nebulae, H II regions). In such cases, the fluorescence will deplete the ($v = 2$, $J = 6$) level of H_2, resulting in observable deficiencies of the infrared lines out of that state.

A more challenging set of H_2 observations is provided by many quasar absorption systems (Weymann et al. 1981). Aaronson et al. (1974) identified 5 of 200 absorption lines in PHL 957 ($z_{em} = 2.69$) with strong H_2 lines at redshift $z_{abs} = 2.309$. Although others have reanalyzed spectra of this quasar (Coleman et al. 1976, Wingert 1975), the confirmation of this detection awaits future data of improved quality. More recently, Levshakov & Varshalovich (1979) identified more than 20 absorption lines in a spectrum obtained by Baldwin et al. (1974) of OQ 172 ($z_{em} = 3.53$) as H_2 Lyman and Werner bands at $z_{abs} = 3.092$ and 2.651. However, only 5 of their identifications agree within ±2 Å (Black 1980). This object contains so many absorption lines that the H_2 identifications may be suspect.

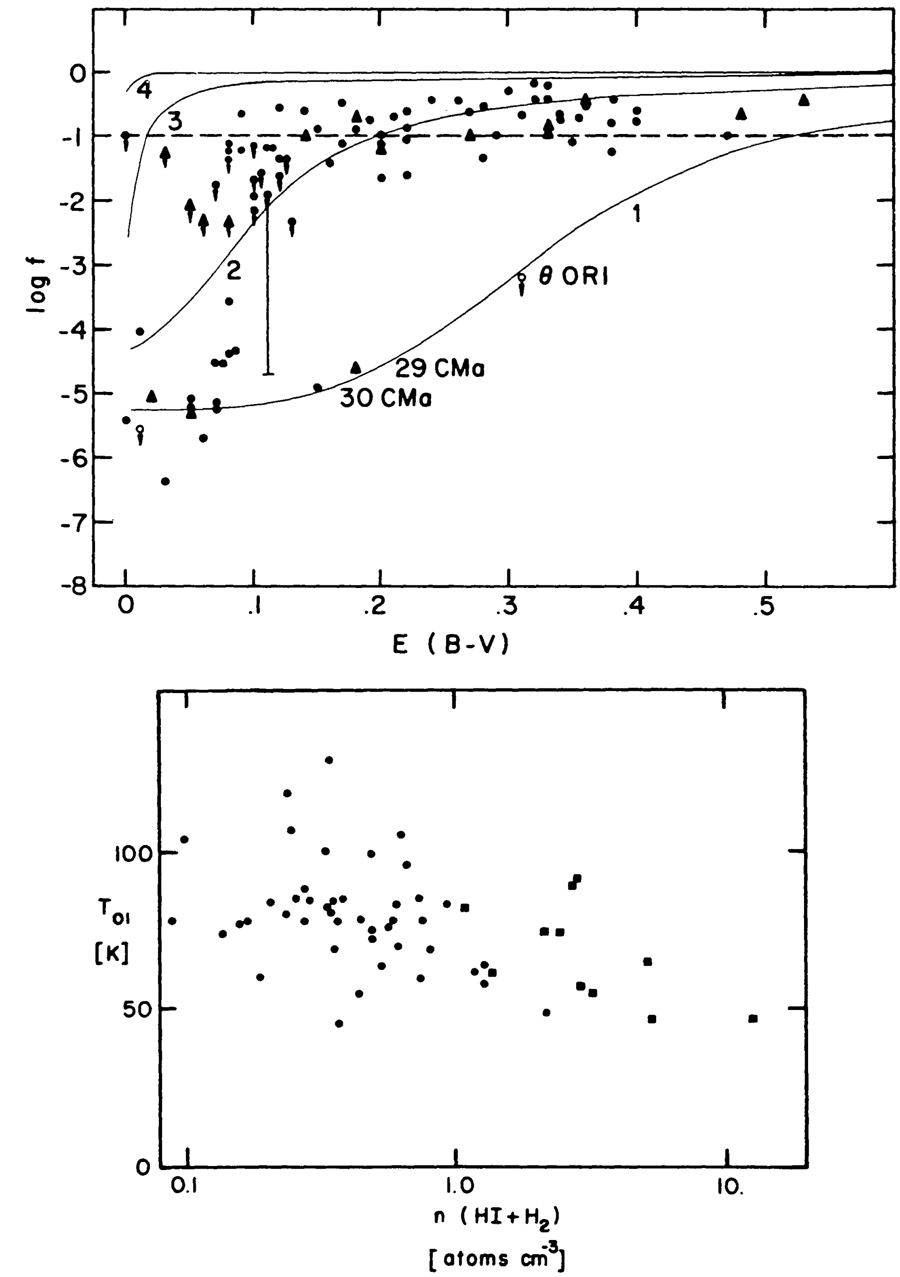

Figure 3 Results of *Copernicus* uv interstellar H_2 survey (Savage et al. 1977). (*top*) Molecular fraction, $f = 2N(H_2)/[N(\mathrm{H\ I}) + 2N(H_2)]$, versus color excess E(B-V) (solid lines denote theoretical models of cloud shielding by Black). (*bottom*) Rotational temperature, T_{01} (from $J = 0$ and 1 column densities), versus average line-of-sight density, $N(H_{tot})/D$.

Higher resolution studies of quasar absorption spectra will yield valuable information on physical conditions in the absorbing clouds. With the current signal-to-noise and spectral resolution, the line identification is difficult, and one cannot perform the key test of identifying lines from individual J states. Some of the absorption lines shortward of 1120 Å (rest frame), often attributed to Lα clouds (Sargent et al. 1980), could arise from H_2 in intervening galaxies. Because the projected area of a spiral galaxy's disk is much less than that of the halo, the large molecular clouds expected to provide strong H_2 lines would be less frequent absorbers than the atomic metal-line systems.

4.2 *Infrared Observations*

Under normal circumstances in interstellar clouds, the temperatures are too low to produce significant column densities of molecules in any but the lowest rotational states. A substantial fraction of the molecules may be excited into vibrational or high rotational states by uv radiation produced by hot stars (Gould & Harwit 1963) or in the transient high-temperature regions behind strong shock waves (Field et al. 1968). The first serious searches for vibrationally excited H_2 (Werner & Harwit 1968, Gull & Harwit 1971) toward dark clouds in the vicinity of hot stars failed to detect H_2 emission. The first two detections of vibrationally excited H_2 appeared in spectra of the infrared cluster in Orion and the planetary nebula NGC 7027 (Gautier et al. 1976, Treffers et al. 1976). Table 2 lists the H_2 sources known at this time.

For most of these objects, the H_2 observations are limited to line fluxes from a few spatial positions; the line intensities are at least an order of magnitude less than those in Orion. The most luminous of these sources are extended regions of H_2 emission near embedded protostars, often accompanied by highly supersonic gas flows within molecular cloud cores. Although the extent of emission in NGC 7538, DR 21, and NGC 6334 is $\sim$1 pc (considerably greater than Orion), and the luminosities are comparable to that of Orion, the line intensities are typically an order of magnitude weaker. When observed, the linewidths of molecular cloud sources are wide. In NGC 2071, the H_2 lines indicate velocities out to 50 km s^{-1} with respect to the majority of the cloud material (Persson et al. 1981). The relatively small sizes and high velocities imply dynamical lifetimes of 10^4 years or less (Beckwith 1981).

Radio wavelength observations for several of the sources show evidence for highly supersonic molecular velocities. It appears that H_2 is excited preferentially in these high-velocity regions, whereas only a small fraction of CO emission appears at high velocity. A number of major uncertainties about the intensity, temperature, line luminosity, and velocity of most of these sources will presumably be resolved by observations in the next several years.

Elias (1980) detected H_2 emission from a large fraction of a limited sample of Herbig-Haro objects in the southern hemisphere. These objects are typically associated with dark clouds; their optical and uv spectra suggest excitation by shocks of 60–120 km s^{-1} (Schwartz & Dopita 1980). Elias' observations suggest that the excitation is thermal rather than radiative, although the observations are unambiguous for only a few objects. Emission lines from H_2 appear in the spectra of the star T Tauri (Beckwith et al. 1978b), but the emission from this object may come from a small Herbig-Haro object (Burnham's nebula) very close to the star. Four other T Tauri stars showed no H_2 lines.

It is interesting to note that H_2 emission is not confined to molecular clouds. While NGC 7027 is not in a particularly dense molecular region, this planetary nebula is associated with a small cloud of molecules probably produced by the central star in its latter stages of evolution (Mufson et al. 1975). The H_2 may

Table 2 Infrared emission line sources[a]

Object	α(1950)			δ(1950)			I	R	References[b]
NGC 1068	02	40	07.1	−00	13	31	2	8	19
T Tau	04	19	04	19	25	00	6	5	4
CRL-618	04	39	33.8	36	01	15	3	10	6, 20
OMC-1	05	32	46.3	−05	24	03	100	4	2, 3, 7, 14, 15, 17
HH-40	05	32	55	−06	20	16	0.5	15	9
OMC-2	05	32	59.6	−05	11	32	0.5	34	11
HH-1	05	33	55	−06	47	02	0.2	15	9
HH-2	05	34	00	−06	49	00	1	10	9, 11
NGC 2071	05	44	31.2	+00	20	48	2	7	1, 16
IC 443	06	14	43	22	23	00	4	10	21
GL 961	06	31	58.9	04	15	07	0.5	15	1
HH-46	08	24	17	−50	50	34	0.09	15	9
HH-53	12	51	35	−76	41	17	0.2	15	9
HH-54B	12	52	10	−76	40	08	1	15	9
NGC 6334	17	16	39.2	−35	54	49	0.5	34	10, 23
NGC 6720	18	51	44	32	57	42	1	10	6
W 51	19	21	22.5	14	25	13	1	6	8
BD + 30° 3639	19	32	47.6	30	24	17	2	10	6
DR 21	20	37	21.9	42	09	18	0.8	34	11
CRL 2688	21	00	19.9	36	29	45	1	10	6
NGC 7027	21	05	09.4	42	02	03	10	5	5, 22
Ceph A	22	54	24.0	61	46	11	1	15	1
NGC 7538	23	11	36.8	61	12	19	0.9	34	12
Hb 12	23	23	57.2	57	54	24	2	10	6

[a] H_2 emission sources as of October, 1981. Columns are as follows: R. A. and Decl. (1950 epoch); I = peak intensity of (1-0) $S(1)$ line in 10^{-4} erg cm^{-2} s^{-1} sr^{-1}; R = resolution (arcsec)

[b] References: (1) Bally & Lane (1982); (2) Beck et al. (1982); (3) Beckwith et al. (1982b); (4) Beckwith et al. (1978b); (5) Beckwith et al. (1980); (6) Beckwith et al. (1978a); (7) Beckwith et al. (1978c); (8) Beckwith & Zuckerman (1982); (9) Elias (1980); (10) Fischer (1981); (11) Fischer et al. (1980a); (12) Fischer et al. (1980b); (13) Gautier (1978); (14) Gautier et al. (1976); (15) Nadeau et al. (1982); (16) Persson et al. (1981); (17) Scoville et al. (1982); (18) Smith et al. (1981); (19) Thompson et al. (1978); (20) Thronson (1981); (21) Treffers (1979); (22) Treffers et al. (1976); (23) Fischer et al. (1982).

be excited by shock waves as the nebula expands into the surrounding cloud. Several other planetary nebulae exhibit H_2 emission (Beckwith et al. 1978a), suggesting that some molecules may often be present in these objects. Perhaps the most remarkable discovery of H_2 emission is in NGC 1068, a Seyfert galaxy observed by Thompson et al. (1978) and Hall et al. (1981). A substantial amount of the molecular material in the nucleus of this galaxy must harbor regions of vibrationally excited H_2 in order to produce observable emission (Beckwith 1981).

The area of the galactic plane that has been surveyed for H_2 emission is still very small. Several limited surveys of sources appear in the literature (Gautier 1978, Beckwith 1978, Scoville et al. 1979, Fischer 1981) in addition to upper limits on various objects (Table 2). Because these searches are limited to rather narrowly defined criteria, it is difficult to draw any firm conclusions about the nature of H_2 emission sources. However, a few general principles for search strategies might be inferred from the limited sample. Many of the luminous H_2 sources in molecular clouds are quite extended (of order of arcmins) compared to typical infrared beamsizes on large telescopes. The most successful surveys employ large beamsizes, which are sensitive to extended, low surface-brightness emission. Many of the objects in molecular clouds also contain regions of highly supersonic velocity flows, which appear to be associated with the H_2 emission. High-velocity wings on CO profiles or H_2O masers may be necessary (but not sufficient) criteria for H_2 emission in dense clouds. Even the Herbig-Haro objects and planetary nebulae have supersonic velocity fields, which might be intimately tied to the excited H_2. Although many of the objects in Table 2 produce copious uv radiation, the correlation between uv and H_2 is much poorer than the correlation between high gas velocities and H_2.

To show how physical conditions within the emitting regions follow from the line observations, it is useful to choose one object as an example. The emission region in Orion is spatially extended and centered on a cluster of infrared stars near the densest part of the cloud (Grasdalen & Joyce 1976, Beckwith et al. 1978c). Figure 4 shows a map of the intensity of the 1-0 $S(1)$ line. The center of the H_2 emission is roughly coincident with the center of the molecular outflow indicated by the millimeter radio observations (Zuckerman et al. 1976, Kwan & Scoville 1976, Genzel et al. 1981). Nadeau & Geballe (1979) showed that the H_2 linewidths are $\sim$50 km s^{-1}, with wings out to 90 km s^{-1} relative to the majority of gas in the cloud. Several recent studies of the kinematic structure of the H_2 emission (Beck et al. 1979) show that the widest lines appear toward the center, whereas the lines near the edges are significantly narrower, as expected if the velocity field is produced by radial outflow. The near-infrared vibrational line profiles toward the center are noticeably asymmetric, being considerably stronger in the blue wings. The (0-0) $S(2)$ line is symmetric, suggesting that the asymmetry in the (1-0) line results from internal reddening.

The relative level populations indicate that the hydrogen molecules are approximately in thermal equilibrium. While it is possible, in principle, to determine the relative H_2 level populations from observations of the intensity of the transitions from those levels, the analysis is complicated by dust absorption effects. Because H_2 rotational transitions emit optically thin quadrupole radiation, dust absorption is more important than self-absorption. The intensity of a transition from i to j can be written as

$$I_{ij} = (A_{ij}\, E_{ij}\, N_i\, e^{-\tau})/4\pi \text{ erg s}^{-1} \text{ cm}^{-2} \text{ sr}^{-1}, \tag{2}$$

where A_{ij} is the spontaneous emission rate (s^{-1}), E_{ij} is the transition energy, N_i is the column density (cm^{-2}) of molecules in state i, and τ is the dust optical depth at energy E_{ij}. Since A_{ij} and E_{ij} are known, and I_{ij} is observed, the column density in level i can be determined once τ is estimated.

The dust opacity is determined by measuring the intensities of two lines at different frequencies and exploiting the frequency dependence of interstellar extinction. Estimates of the 2 μm opacity vary from about one to four magnitudes toward the H_2 emission in Orion, depending on the lines used, the spatial resolution, and the point in the nebula. The earliest observations by Beckwith et al. (1979) and Simon et al. (1979) gave a value $\tau_1 = 4$ for the opacity, τ_1, at the 2.1 micron wavelength of the 1-0 $S(1)$ line. More refined

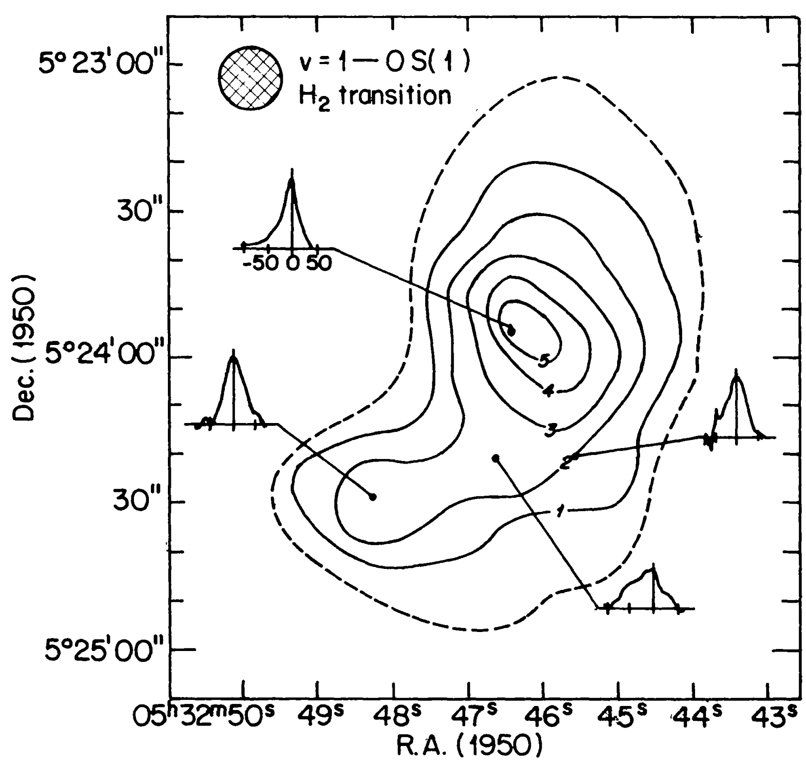

Figure 4 Distribution of 2μm vibrational H_2 emission in Orion (Beckwith et al. 1978c). Line profiles from several positions (Nadeau et al. 1982) are normalized to same peak intensity. For an assumed distance of 500 pc, one arcmin corresponds to 0.15 pc.

observations by Scoville et al. (1982), using essentially the same lines and assumptions, bring the estimate down to $\tau_1 = 1$–2. Still different pairs of lines yield estimates $\tau_1 = 2$–2.5 (Beckwith et al. 1982a) and $\tau_1 = 2.2$–4.0 (Knacke & Young 1981). The technique used by Knacke & Young is subject to considerable systematic error, owing primarily to uncertainties in the temperature distribution of the gas. It is clear, however, that the dust opacity to the H_2 emission in Orion (and quite likely other molecular clouds) is substantial and affects the vibration-rotation line intensities by a factor between three and forty.

In addition to uncertainties in the observations and in the extrapolation from selective to total extinction, there may be considerable opacity distributed throughout the emission region. In fact, the predominance of blue-shifted velocities in the H_2 line profiles may arise from an expanding dusty emission region in which the red-shifted molecules suffer more extinction than the blue-shifted ones (Nadeau & Geballe 1979, Nadeau et al. 1982). Because of uncertainties in the distribution of extinction, it may be impossible to compare the intensities of several lines at different wavelengths, or to derive the total luminosity of any one line without assuming a specific model for the structure of the emission region.

Using a typical value for τ_1, one may compare the relative column densities with the Boltzmann relation to derive the molecular temperature. The molecules appear to be approximately thermalized at a temperature range of 500 to 3000 K; the higher temperature applies to the higher energy levels. Most authors use 2000 K to characterize the emission from the $v = 1$ and 2 states. The temperature derived from the (1-0) and (2-1) lines is insensitive to τ_1. In general, an uncertain distribution of temperatures complicates the emission analysis as much as does the uncertain form of the extinction curve, particularly for the (0-0) $S(2)$ line (Beck et al. 1979), which is dominated by gas cooler than 1000 K.

The total luminosity of the emission and the mass of the hot H_2 can be estimated from the temperature, column density, and spatial distribution of the emission. The intensity map (Figure 4) determines the total number of molecules in the ($v = 1$, $J = 3$) level when Equation (2) and the extinction are used. The number of molecules in other states follows from the Boltzmann relation at an appropriate temperature. The best current estimates for the luminosity and mass of the vibrationally excited molecules are 150 $L_\odot$ and 0.03 $M_\odot$ (Scoville et al. 1982, Beckwith et al. 1982a). Uncertainties in the dust opacity have a far greater effect than those in temperature for determining the luminosity. The mass of the emitting H_2 is small compared to the total mass of the central region. The luminosity of the hot H_2 is considerable, however, and may constitute the primary cooling mechanism for shock waves in the cloud core.

The observations of most H_2-emitting clouds are limited to the intensity of the 1-0 $S(1)$ line in a few positions only; often maps of this line are nonexistent or grossly undersampled. Estimates of the temperature and extinction exist for a few sources, based on less systematic measurements than those for Orion. Although the best estimates of temperature are derived from the intensity of the (2-1) $S(1)$ line—typically 10% of (1-0) $S(1)$—this line is often too weak for practical observations. Upper limits to this line intensity are consistent with gas at a few thousand degrees. The ortho- to para-hydrogen ratios are consistent with the statistical equilibrium value of three.

5. THEORIES OF EXCITATION

The detection of H_2 in excited rotational, vibrational, or electronic states can be a valuable diagnostic of conditions in the interstellar medium, but only if the source of excitation is known. In this section, we discuss several excitation mechanisms, divided into the categories of thermal and nonthermal processes.

5.1 *Thermal Excitation*

Orion is the best studied of the H_2 IR-emission sources. The relative level populations indicate a region in approximate thermal equilibrium with $T \sim 2000$ K, while the line profiles exhibit velocities up to 90 km s^{-1}. These observations, together with the theoretical considerations of explaining such a source of heating or excitation, have been taken as evidence of shock waves originating in the cores of the Orion (and other) molecular clouds.

Initially, the Orion data were explained by simple models of steady, plane-parallel shocks in molecular clouds (Hollenbach & Shull 1977, Kwan 1977, London et al. 1977). These models are characterized primarily by two parameters: the preshock density n_0 (molecules cm^{-3}), and the shock velocity V_s (km s^{-1}). The magnetic field B_0 and fractional ionization play minor roles in these models. Collisional dissociation of H_2 becomes important for $V_s > 15$ km s^{-1} if $n_0 \gtrsim 10^{5-6} cm^{-3}$. Viewing the shock in the frame in which the front is at rest, one may delineate four zones: (*a*) the preshock zone, irradiated by a possible uv precursor; (*b*) the region in which the preshock directed flow is randomized into thermal (translational) energy; (*c*) the region in which rotational and vibrational states are collisionally excited; and (*d*) the region in which the postshock gas is radiatively cooled and compressed. Because the H_2 elastic cross sections are one or two orders of magnitude greater than the inelastic cross sections, region (*b*) may be assumed to be a discontinuity in temperature and density. At high density ($n_0 \gtrsim 10^5$ cm^{-3}), region (*c*) may also be treated as a discontinuity, in which a thermal population of rotational and vibrational states is produced before the H_2 loses appreciable energy through radiation. At low densities, regions (*c*) and (*d*) are coincident, since each inelastic collision results in a significant radiative loss.

Adopting the usual adiabatic jump conditions, one may estimate the postshock temperature in region (*c*) to be

$$T_s = \frac{2(\gamma-1)}{(\gamma+1)^2}\frac{\mu V_s^2}{k} \cong (3080\ \mathrm{K})\left(\frac{V_s}{10\ \mathrm{km/s}}\right)^2, \tag{3}$$

where μ is the mean molecular weight of the postshock gas (2.33 m_H, including 10% He) and γ is the adiabatic index (assumed to be 9/7 for three translational, one vibrational, and two rotational modes). The postshock cooling proceeds through the collisional excitation and radiative decay of infrared emission lines of H_2 [optically thin for column densities $N(H_2) \leq 10^{24}\ \mathrm{cm^{-2}}$]; OI, CO, OH, and H_2O can be important high-density coolants for temperatures below 10^3 K (Hollenbach & McKee 1981, Draine et al. 1982). The intensity I_{ij} (erg cm^{-2} s^{-1} sr^{-1}) of an optically thin H_2 line is given by Equation (2) in the previous section. We may estimate this intensity by assuming the molecules to be at the postshock temperature T_s for a cooling time

$$t_c = \left(\frac{\gamma}{\gamma-1}\right)\frac{kT_s}{f_i\, A_{ij}\, E_{ij}\, \gamma_{ij}}. \tag{4}$$

Thus, $N(H_2) \approx n_o V_s t_c$, where γ_{ij} represents the ratio of the total cooling rate to the rate in the line (ij). Using Equation (3), we then obtain

$$I_{ij} \approx \frac{\mu n_0 V_s^3}{4\pi\gamma_{ij}}\left(\frac{2\gamma}{(\gamma+1)^2}\right). \tag{5}$$

Thus, for shocks with thermal level productions, the absolute H_2 line intensities determine the product $n_0 V_s^3$, while the relative line intensities fix V_s (through the temperature dependence of γ_{ij}). If the preshock density is less than 10^5 cm^{-3}, γ_{ij} depends on both n_0 and V_s, since A_{ij} exceeds the collisional de-excitation rate. To fit the Orion absolute intensities, we require $n_0 \gtrsim 2 \times 10^6$ cm^{-3} for $V_s \sim 10$ km s^{-1} and two magnitudes of extinction at 2.1 μm. The relative line intensities [principally the ratio of (2-1) $S(1)$ to (1-0) $S(1)$] fix $V_s \approx 10$ km s^{-1} if collisional dissociation is negligible. However, as Kwan (1977) and London et al. (1977) point out, the intensities of the (1-0) and (2-1) lines in high-density shocks vary little for shock velocities between 10 and 25 km s^{-1}, because the 2μm line emission occurs at essentially the same temperature range (1000–4000 K) owing to the strong postshock dissociational cooling. Above 25 km s^{-1}, the H_2 is completely dissociated for high-density shocks (Hollenbach & McKee 1980).

Because of the dissociation problem, the 90 km s^{-1} wings in many H_2 emission lines cannot be explained by the simple shock models. Efforts to explain this high-velocity emission have fallen into three classes: (*a*) H_2 re-formation models; (*b*) magnetic precursor models; and (*c*) high-velocity "blob" models. We discuss each of these mechanisms in turn.

Hollenbach & McKee (1979) suggest that in shocks with $V_s > 25$ km s^{-1}, the dissociated H_2 might re-form on grains in the cool post-shock layer if a substantial fraction of grains survive the shock (Draine & Salpeter 1979). The vibrational emission in this model results primarily from formation-pumping (see Section 4.1), for which the degree of excitation is uncertain. Some thermal excitation may be needed to mimic the observed 2000 K level populations. At very large densities, formation-heating and radiation-trapping could raise the gas temperature sufficiently to produce some vibrational excitation. However, this mechanism is unlikely in Orion, with only two magnitudes of extinction at 2 μm.

Draine (1980) has discussed the importance of magnetic precursors in low-velocity interstellar shocks. If the fractional ionization is low, ion-neutral collisions are insufficient to couple the neutrals to the ion-electron fluid (Mullan 1971). Consequently, the magnetic field is not frozen to the gas. If the ion-electron fluid can propagate magnetosonic disturbances at a velocity

$$V_{\text{ims}} = \left\{ \frac{[B^2/4\pi + 5(n_e + n_i)kT/3]/(\rho_e + \rho_i)}{1 + B^2/4\pi(\rho_e + \rho_i)c^2} \right\}^{1/2} \tag{6}$$

exceeding the shock speed V_s, then the magnetic field may be compressed and accelerated ahead of the neutral shock front, over a damping length

$$L \approx \frac{(\mu_n + \mu_i)B_0^2}{\pi\rho_{io}\,\rho_{no}\langle\sigma V\rangle V_s}. \tag{7}$$

Here, (μ_n, ρ_n) and (μ_i, ρ_i) are the mass and mass density of the neutrals and ions, respectively, and $\langle\sigma V\rangle$ is the rate coefficient for ion-neutral momentum exchange. In this precursor, the ions and electrons stream through the neutrals, depositing their heat through damping of the magnetosonic waves. Both the streaming and the neutral heating may excite H_2 vibrational emission. Furthermore, such shocks may remain nondissociative to velocities somewhat above 25 km s^{-1}. If the preshock magnetic field B_0 is larger than a critical value B_{cr} (which depends on the postshock cooling rate), the magnetic precursor will "quench" the neutral shock, allowing the neutral flow variables to be continuous everywhere.

In Orion, if the preshock gas has a density $n_0 \approx 10^6$ cm^{-3}, a magnetic field of $\sim 2 \times 10^{-3}$ G could produce sufficient ion-neutral decoupling and neutral heating, which would explain the observed line intensities (Draine et al. 1982). However, for $V_s > 50$ km s^{-1}, the ions and electrons produced by collisional ionization will dissociate the H_2, as well as couple the ions and neutrals. Therefore, magnetic precursors still do not explain the 90 km s^{-1} H_2 line wings. In addition, the existence of milligauss fields in the Orion cloud has yet to be demonstrated.

The third type of model proposed for the Orion emission might be termed the "blob" model (Chevalier 1980, Shull 1982). Kuiper et al. (1981) and

Nadeau et al. (1982) have argued on the bases of radio (CO) and IR (H_2) data, respectively, that outflowing density inhomogeneities are required to explain the Orion line profiles. In this picture, the high-velocity H_2 wings are produced by dense blobs in a general outflow. The H_2 line width is determined by the bulk flow, whereas individual blobs contain nondissociative shocks of lower velocity (with possible magnetic precursors). This hybrid shock model would explain why the centroid of the high-velocity emission has the same velocity as the ambient molecular cloud (Knapp et al. 1981). The asymmetric H_2 emission in the blue wings would result from extinction from the back sides of receding blobs.

The case for the ejection of high-velocity condensations from protostars in molecular clouds has been made by many authors (e.g. Norman & Silk 1978, Cantó & Rodríguez 1980). With masses $\sim 10^{-4} M_\odot$, these condensations may appear in the form of high-velocity H_2O masers, Herbig-Haro objects, and H_2-emitting blobs. The source of these ejecta is uncertain because the momentum in the molecular outflows from these regions is several orders of magnitude greater than the single-scattering momentum, L/c, in the radiation field. Suggested mechanisms (Shull 1982) include a mechanically driven stellar wind, a pulsational instability of the protostar (η Carinae phenomenon), magnetic torques, centrifugal forces, or a gravitational slingshot during the breakup of a protocluster.

5.2 *Nonthermal Excitation*

Molecular hydrogen may be excited nonthermally by absorption of uv photons (Section 4.1), by collisions with high-energy electrons, or by resonance fluorescence of H_2 with Lα, Lβ, and other lines. The strength of the uv continuum radiation is usually parametrized by its ratio to the average interstellar flux near 1000 Å (Habing 1968, Jura 1974), $F_0 = (10^5$ photons cm^{-2} s^{-1} Å$^{-1})$. The unshielded H_2 absorption rate in the Lyman and Werner bands for a uv flux F may be written $\beta = \beta_0(F/F_0)$, where $\beta_0 = 5 \times 10^{-10}$ s^{-1} (Jura 1974). In the cloud interior, the absorption rate is reduced by dust absorption and line self-shielding,

$$\beta(N_2) = \beta_0(F/F_0)\exp(-\tau_d)f(N_2), \tag{8}$$

where τ_d is the dust absorption optical depth at 1000 Å, N_2 is the H_2 column density into the cloud, and $f(N_2)$ is a line self-shielding factor (Jura 1974, Shull 1978a, Federman et al. 1979).

Approximately 11% of the Lyman and Werner band absorptions lead to dissociation, and the remainder to uv fluorescence and IR radiative cascade through bound states, vJ, of the ground electronic state. For every cascading molecule, there is typically a one to three percent chance that it will "flow" through a particular line in the (1-0) band. At low densities and uv fluxes, the radiative cascade is entirely determined (Black & Dalgarno 1976) by the product of the "cascade entry matrix" (the fraction of pumped H_2 that enters the ground electronic state in level vJ) with the "cascade efficiency arrays" (which describe the cascade lines that result per unit population rate of level vJ).

The column density in an excited state (and hence, the emission line fluxes) may be estimated (Hollenbach & Shull 1977) by multiplying the total rate of H_2-pumping in that column, P_T (cm^{-2} s^{-1}), by $\xi(vJ)\tau(vJ)$, where ξ is the fraction of pumped H_2 that passes through vJ, and where τ is the radiative lifetime of vJ. Assuming that most of the pumped H_2 lines lie on the "square root" portion of the curve of growth and neglecting dust extinction, one finds that

$$P_T = (4.6 \times 10^6)(F/F_0) \text{ pumps cm}^{-2}\text{ s}^{-1}. \tag{9}$$

The factors ξ and τ are given by Black & Dalgarno (1976), Shull (1978a), and Turner et al. (1977).

A full treatment of the population rate of the H_2 levels must often include other processes that interrupt the purely radiative cascade. Collisions with H I or H_2 will de-excite low rotational states in cool clouds when $n \gtrsim 10$ cm^{-3}. Vibrational levels will be affected at densities exceeding 10^{5-6} cm^{-3}, depending on the temperature. Ultraviolet radiation will interrupt the cascade by "multiple pumping" when $(F/F_0) \gtrsim 10^4$.

The Orion IR emission would require uv fluxes $(F/F_0) > 10^6$ to explain the (1-0) $S(1)$ line intensity if there were no dust extinction (Hollenbach & Shull 1977). However, the cascade efficiencies predict the (2-1) $S(1)$ line to be of comparable strength, rather than in the observed ratio of 0.1 (Beckwith et al. 1978c). Furthermore, multiple pumping and dust absorption greatly reduce the vibrational pumping efficiency ξ in the extreme uv fields required for Orion (Shull 1978a, London 1978). A related problem is that dust grains may be too hot to catalyze the formation of H_2. Therefore, it is unlikely that the Orion source is excited by uv-pumping.

Nonthermal excitation of H_2 by high-energy electrons most commonly results when a molecular cloud is exposed to a strong source of penetrating X rays. Photons of energy greater than about 0.6 keV are absorbed in photoionization of trace heavy elements in the gas and grains (Fireman 1974). The resulting secondary electrons (Shull 1980a) lose their energy in further H_2 ionizations, dissociations, and excitations (Glassgold & Langer 1973), Cravens et al. 1975, Douthat 1979). The latter work, which uses cross sections of Gerhart (1975), finds that a 10 keV photoelectron released in a cold molecular cloud deposits its energy primarily in H_2^+ ionizations (~46%), Lyman and Werner excitations (~20%), dissociating triplet excitations (~10%), and IR-line excitations (~10%). The uv lines are absorbed by dust and reradiated as

IR continuum, while the H_2^+ ions deposit heat through dissociative collisions with H_2 or electrons.

Lepp & McCray (1982), in a study of the temperature structure and nebular emission of X-ray-illuminated molecular clouds, show that ~20% of the absorbed X-ray luminosity may be reradiated in (0-0) and (1-0) vibrational lines, excited primarily by thermal collisions with X-ray-heated gas. The coexistence of H_2 and a strong X-ray flux might be expected near binary X-ray sources embedded in molecular clouds, outside buried supernovae (Shull 1980b, Wheeler et al. 1980), or in the cores of active galaxies. Perhaps some of the 2 μm emission in the Seyfert galaxy NGC 1068 is produced in this fashion. Quasars and BL Lac objects could be H_2 sources if clouds of sufficiently large column density exist in their inner regions.

6. FUTURE WORK

6.1 *Ultraviolet Observations*

The *Copernicus* satellite made many contributions to our understanding of interstellar H_2 and physical conditions in diffuse clouds. However these data have raised new questions and have pointed the way toward observations that should be made in the future. While *IUE* (International Ultraviolet Explorer) and the *Space Telescope* will extend interstellar studies to more distant, reddened stars, they lack the far-uv sensitivity necessary for thorough studies of H_2. (The Space Telescope High Resolution Spectrometer may be able to study the 0-0 and 1-0 Lyman lines near 1100 Å.) For this and many other reasons, astronomers anticipate the development of a far-uv spectroscopic Explorer satellite (*FUSE*).

What are the requirements of such a telescope-detector system relevant to the study of interstellar H_2? First, the wavelength coverage should extend down to ~ 930 Å to detect the strong H_2 Lyman lines. Second, the spectral resolution, $\lambda/\Delta\lambda$, should be at least 10^5 ($\Delta V = 3$ km s^{-1}) in order to separate the various blended clouds along the line of sight and to place the uv interstellar observations on an equal footing with optical studies of CH^+ (Federman 1980), Ca II and Na I (Hobbs 1978), and Ti II (Stokes 1978), and with 21-cm studies of H I (Giovanelli et al. 1978). Third, the far-uv detectors should be capable of observing stars of 9–10^m with E(B-V) up to 2.0^m. This capability will extend interstellar studies to stars more distant than 1 kpc and will help bridge the gap between studies of diffuse and molecular clouds. Finally, the instrument should be able to measure weak absorption features (~1 mÅ equivalent width), especially important for lines from H_2 ($J = 4$ and 5) levels.

What new science is *FUSE* likely to uncover? High-resolution data will alter the interpretation of physical conditions in the H_2 absorption features that are blended in most *Copernicus* spectra. Molecular hydrogen provides too important a diagnostic of kinetic temperature, hydrogen density, and uv radiation field to dilute the line-of-sight information by inadequate spectral resolution. The extension of H_2 studies to more distant stars may yield important information on overall galactic properties: metallicity gradients, cosmic-ray heating and ionization rates, dust-to-gas ratios, uv radiation fields, and kinetic temperatures.

It will be useful to search for H_2 toward late B- and A-type stars, in order to distinguish true interstellar H_2 from that associated with shells around OB stars. Because the kinetic temperature of diffuse clouds, the molecular fraction of hydrogen, and the H_2 rotational excitation may all be affected by shock heating and uv radiation near OB stars, the uv observations of A stars may probe an entirely new class of diffuse clouds (seen perhaps in 21-cm absorption-emission comparisons). We need to know whether the heat sources required to explain the *Copernicus* H_2 rotational temperatures ($\langle T_{01} \rangle \approx 80$ K) are a general phenomenon in the interstellar medium (Spitzer 1978), or reflect an observational bias toward gas near hot stars.

The *FUSE* spectrometer may also yield data on gas in dark interstellar clouds, where the greater molecular fractions, diminished uv radiation fields, and altered dust properties may affect the H_2 rotational excitation and kinetic temperature. These studies will provide reliable CO/H_2 ratios (crucial for mass determinations of these clouds), as well as temperature, density, and velocity profiles in the transition regions between the warm atomic cloud envelopes and the cold cloud cores. The uv detection of trace molecular species in these transition regions will provide further links between optical uv diffuse cloud astronomy and IR/radio molecular cloud astronomy.

Some of the most exciting prospects for uv H_2 spectroscopy lie in extragalactic astronomy. By sacrificing spectral resolution for sensitivity, one might use distant uv sources (high-latitude stars, globular clusters, Seyfert galaxies, or quasars) to probe outlying clouds in our Galaxy or in nearby spiral galaxies. Although these data would yield average physical properties of interstellar matter, this would be extremely useful in studies of galactic chemical and luminosity evolution and in the developing field of extragalactic CO radio astronomy (Elmegreen et al. 1980).

The reliable detection of H_2 in absorption line systems toward quasars has the potential of triggering a breakthrough in understanding the physical nature and location of these systems. For low-redshift quasars, the task of achieving the full benefits of the H_2 diagnostics will push far-uv technology to its limits (both high sensitivity and high spectral resolution are needed). The probability that a quasar line of sight intercepts a spiral galactic disk increases at large redshift z. High-resolution optical studies ultimately may detect H_2 toward many high-z quasars, providing information on dust, molecules, and physical conditions in star-forming regions at early epochs.

6.2 *Infrared Emission Lines*

Although the detection of H_2 emission has raised many questions, perhaps the most important concerns are how some H_2 molecules survive the strongest shocks and how shock waves affect the evolution of molecular clouds. The question of H_2 survival requires a knowledge of the shock structure, which can perhaps be addressed by measurements of emission lines of H_2 and other molecules at higher spectral and spatial resolution. Such observations may distinguish among competing theoretical models (Section 5.1) by such characteristics as line profiles, velocity shifts, or excitation temperature correlations with velocity.

The effect of shock waves on molecular clouds may be a more fascinating topic. If the winds or explosions that give rise to the shocks are common features of protostellar evolution, they might play a role in maintaining internal velocities in clouds or in limiting the rate of secondary star formation (Norman & Silk 1980, Beckwith 1981). A reasonable estimate of the stellar birthrate will require well-sampled surveys of strong molecular shocks and estimates of the fraction of shock energy transmitted to cloud turbulence.

Probably the most important H_2 line observations will be of the cooler molecules that constitute the majority of cloud mass. Unfortunately, the lowest emitting levels are weakly populated at typical cloud temperatures ($J = 2$ has an excitation energy of 510 K, compared with dense cloud temperatures ~ 50 K). Calculations of the emissivities of the lowest IR transitions (Dalgarno & Wright 1972, Drapatz & Michel 1974, Bussoletti & Stasinska 1975) indicate that these H_2 lines are marginally detectable with existing technology. However, the lines may be difficult to distinguish from the strong dust continuum (Drapatz & Michel 1974). Detection of these lines will require extremely high photometric sensitivity and spectral resolution consistent with the cloud velocity fields of several km s^{-1} ($\lambda/\Delta\lambda \cong 10^5$).

The two lowest rotational transitions at 28 and 17 μm, as well as many vibration-rotational transitions, occur in regions with strong telluric absorption. The detection of these lines at balloon or airborne altitudes would be desirable for extinction curve determinations, as well as to assess the value of observations from space. Ultimately, orbiting observatories such as *SIRTF* (Shuttle Infrared Telescope Facility) will provide an enormous increase in sensitivity for H_2 detection.

While we have concentrated entirely on H_2 in this article, we should mention the importance of the isotopic form HD, which can be detected in uv absorption and IR emission. With an appropriate correction for chemical fractionation, a measurement of the ratio HD/H_2 in dense clouds could yield the cosmologically important D/H ratio. The higher dipole transition rates of HD partially offset its decreased abundance relative to H_2. Therefore, it may eventually be possible to detect HD emission in the same objects in which H_2 is now seen.

ACKNOWLEDGMENTS

We are grateful to J. Black, A. Dalgarno, B. Draine, N. Evans, D. Hollenbach, M. Jura, S. Leone, S. Lepp, C. F. McKee, F. Palla, E. Salpeter, L. Spitzer, and I. Wasserman for helpful suggestions during the preparation of this review. Our work was supported by grants from NSF (AST80-19960) and NASA (NSG-2412).

Literature Cited

Aannestad, P. A. 1973a. *Ap. J. Suppl.* 25:205–22
Aannestad, P. A. 1973b. *Ap. J. Suppl.* 25:223–52
Aannestad, P. A., Field, G. B. 1973. *Ap. J. Lett.* 186:L29–32
Aaronson, M., Black, J. H., McKee, C. F. 1974. *Ap. J. Lett.* 191:L53–56
Audibert, M. M., Joffrin, C., Ducuing, J. 1974. *Chem. Phys. Lett.* 25:158–63
Baldwin, J. A., Burbidge, E. M., Burbidge, G. R., Hazard, C., Robinson, L. B., Wampler, E. J. 1974. *Ap. J.* 193:513–23
Bally, J., Lane, A. P. 1982. *Ap. J.* In press
Beck, S. C., Bloemhof, E. E., Serabyn, E., Townes, C. H., Tokunaga, A. T., Lacy, J. H., Smith, H. A. 1982. *Ap. J. Lett.* 253:L83–87
Beck, S. C., Lacy, J. H., Geballe, T. R. 1979. *Ap. J. Lett.* 234:L213–16
Beckwith, S. 1978. PhD thesis. Calif. Inst. Technol.
Beckwith, S., 1981. In *Infrared Astronomy, IAU Symp. No. 96*, ed. C. G. Wynn-Williams, D. P. Cruikshank, pp. 167–98. Dordrecht: Reidel. 376 pp.
Beckwith, S., DeNoyer, L. K., Evans, N. J., Gatley, I., Gull, G., Russell, R. W. 1982a. *Ap. J.* In press
Beckwith, S., Evans, N. J., Gatley, I., Gull, G., Russell, R. W. 1982b. Preprint
Beckwith, S., Gatley, I., Matthews, K., Neugebauer, G. 1978b. *Ap. J. Lett.* 223:L41–44
Beckwith, S., Neugebauer, G., Becklin, E. E., Matthews, K. 1980. *Astron. J.* 85:886–90
Beckwith, S., Persson, S. E., Gatley, I. 1978a. *Ap. J. Lett.* 219:L33–38
Beckwith, S., Persson, S. E., Neugebauer, G. 1979. *Ap. J.* 227:436–40
Beckwith, S., Persson, S. E., Neugebauer, G., Becklin, E. E. 1978c. *Ap. J.* 223:464–70
Beckwith, S., Zuckerman, B. 1982. *Ap. J.* In press
Bieniek, R. J., Dalgarno, A. 1979. *Ap. J.* 228:635–39
Black, J. H. 1978. *Ap. J.* 222:125–31
Black, J. H. 1980. Bok Prize Lecture, Harvard Univ.
Black, J. H., Dalgarno, A. 1976. *Ap. J.* 203:132–42
Black, J. H., Dalgarno, A. 1977. *Ap. J. Suppl.* 34:405–23
Black, J. H., Hartquist, T. W., Dalgarno, A. 1978. *Ap. J.* 224:448–52
Breshears, W. D., Bird, P. F. 1973. *Symp. Int. Combust.* 14:211
Burke, J. R., Hollenbach, D. J. 1980. NASA Tech. Memo 81163. Ames Res. Cent.
Bussoletti, E., Stasinska, G. 1975. *Astron. Astrophys.* 39:177–84
Cantó, J., Rodríguez, L. F. 1980. *Ap. J.* 239:982–87
Carruthers, G. 1970. *Ap. J. Lett.* 161:L81–85
Chevalier, R. 1980. *Astrophys. Lett.* 21:57–61
Chu, S-I., Dalgarno, A. 1975 *Astrophys. J.* 199:637–41
Coleman, G., Carswell, R. F., Strittmatter, P. A., Williams, R. E., Baldwin, J. A., Robinson, L. B., Wampler, E. J. 1976. *Ap. J.* 207:1–15
Cravens, T. E., Victor, G. A., Dalgarno, A. 1975. *Planet. Space Sci.* 23:1059–70
Dalgarno, A., Black, J. H., Weisheit, J. C. 1973. *Astrophys. Lett.* 14:77–79
Dalgarno, A., Kingston, A. E. 1963. *Observatory* 83:39–40
Dalgarno, A., Roberge, W. G. 1979. *Ap. J. Lett.* 233:L25–27
Dalgarno, A., Stephens, T. L. 1970. *Ap. J. Lett.* 160:L107–9
Dalgarno, A., Wright, E. L. 1972. *Ap. J. Lett.* 174:L49–52
Douthat, D. A. 1979. *J. Phys. B* 12:663–78
Dove, J. R., Teitelbaum, H. 1974. *Chem. Phys.* 6:431–44
Draine, B. T. 1980. *Ap. J.* 241:1021–38
Draine, B. T., Roberge, W. G., Dalgarno, A. 1982. *Ap. J.* Submitted for publication
Draine, B. T., Salpeter, E. E. 1979. *Ap. J.* 231:438–55
Drapatz, S., Michel, K. W. 1974. *Astron. Astrophys.* 36:211–16
Eddington, A. S. 1937. *Observatory* 60:99
Elias, J. H. 1980. *Ap. J.* 241:728–36
Elitzur, M., Watson, W. D. 1978. *Astron. Astrophys.* 70:443–46
Elitzur, M., Watson, W. D. 1980. *Ap. J.* 236:172–81
Elmegreen, B. G., Elmegreen, D. M., Morris, M. 1980. *Ap. J.* 240:455–63

Elmegreen, B. G., Lada, C. J. 1977. *Ap. J.* 214:725–41
Federman, S. R. 1980. *Ap. J. Lett.* 241:L109–12
Federman, S. R. 1982. *Ap. J.* 253:601–5
Federman, S. R., Glassgold, A. E. 1980. *Astron. Astrophys.* 89:113–17
Federman, S. R. Glassgold, A. E., Kwan, J. 1979. *Ap. J.* 227:466–73
Field, G. B., Rather, J. D. G., Aannestad, P. A., Orszag, S. A. 1968. *Ap. J.* 151:953–75
Field, G. B., Sommerville, W. B., Dressler, K. 1966. *Ann. Rev. Astron. Astrophys.* 4:207–44
Fink, U., Wiggins, T. A., Rank, D. M. 1965. *J. Mol. Spectrosc.* 18:384–95
Fireman, E. L. 1974. *Ap. J.* 187:57–60
Fischer, J. 1981. PhD thesis. State Univ. New York (Stony Brook)
Fischer, J., Joyce, R. R., Simon, M., Simon T. 1982. Preprint
Fischer, J., Righini-Cohen, G., Simon, M. 1980a. *Ap. J. Lett.* 238:L155–60
Fischer, J., Righini-Cohen, G., Simon, M., Simon, T. 1980b. *Ap. J. Lett.* 240:L95–98
Frisch, P. C., Jura, M. 1980. *Ap. J.* 242:560–67
Gautier, T. N. 1978. PhD thesis. Univ. Ariz.
Gautier, T. N., Fink, U., Treffers, R. R., Larson, H. P. 1976. *Ap. J. Lett.* 207:L129–34
Gentry, W. R., Giese, C. F. 1975. *Phys. Rev. A* 11:90–96
Genzel, R., Reid, M. J., Moran, J. M., Downes, D. 1981. *Ap. J.* 244:884–902
Gerhart, D. E. 1975. *J. Chem. Phys.* 62:821–32
Gerola, H., Seiden, P. E. 1978. *Ap. J.* 233:129–39
Giovanelli, R., Haynes, M. P., York, D. G., Shull, J. M. 1978. *Ap. J.* 219:60–71
Glassgold, A. E., Langer, W. D. 1973. *Ap. J.* 186:859–88
Gold, T. 1961. *Mem. Soc. R. Sci. Liege* 20:476
Goodman, F. O. 1978. *Ap. J.* 226:87–94
Gould, R. J., Harwit, M. 1963. *Ap. J.* 137:694–97
Gould, R. J., Salpeter, E. E. 1963. *Ap. J.* 138:393–407
Grasdalen, G. L., Joyce, R. R. 1976. *Bull. Am. Astron. Soc.* 8:349
Green, S. 1975. *J. Chem. Phys.* 62:2271–77
Green, S., Ramaswamy, R., Rabitz, H. 1978. *Ap. J. Suppl.* 36:483–96
Green, S., Truhlar, D. 1979. *Ap. J. Lett.* 231:L101–3
Gull, T. R., Harwit, M. 1971. *Ap. J.* 168:15–27
Habing, H. 1968. *Bull. Astron. Inst. Neth.* 19:421–31
Hall, D. N. B., Kleinmann, S. G., Scoville, N. Z., Ridgway, S. T. 1981. *Ap. J.* 248:898–905
Herzberg, G. 1950. *Spectra of Diatomic Molecules*. New York: Van Nostrand Reinhold. 658 pp.
Hobbs, L. 1978. *Ap. J.* 222:491–507
Hollenbach, D. J., Chu, S-I., McCray, R. 1976. *Ap. J.* 208:458–67
Hollenbach, D. J., McKee, C. F. 1979. *Ap. J. Suppl.* 41:555–92
Hollenbach, D. J., McKee, C. F. 1980. *Ap J. Lett.* 241:L47–50
Hollenbach, D. J., McKee, C. F. 1981. *Bull. Am. Astron. Soc.* 12:826
Hollenbach, D. J., Salpeter, E. E. 1970. *J. Chem. Phys.* 53:79–86
Hollenbach, D. J., Salpeter, E. E. 1971. *Ap. J.* 163:155–80
Hollenbach, D. J., Shull, J. M. 1977. *Ap. J.* 216:419–26
Hollenbach, D. J., Werner, M. W., Salpeter, E. E. 1971. *Ap. J.* 163:165–80
Huber, J. P., Herzberg, G. 1979. *Constants of Diatomic Molecules*. New York: Van Nostrand
Hughes, M. P., Thompson, A. R., Colvin, R. S. 1971. *Ap. J. Suppl.* 23:323–70
Hunter, D. A., Watson, W. D. 1978. *Ap. J.* 226:477–82
Hutchins, J. B. 1976. *Ap. J.* 205:103–21
Jennings, D. E., Brault, J. W. 1982. *Ap. J. Lett.* In press
Jordan, C., Brueckner, G. E., Bartoe, J-D. F., Sandlin, G. D., Van Hoosier, M. E. 1978. *Ap. J.* 226:687–97
Jura, M. 1974. *Ap. J.* 191:375–79
Jura, M. 1975a. *Ap. J.* 197:575–80
Jura, M. 1975b. *Ap. J.* 197:581–86
Jura, M. 1976. *Ap. J.* 204:12–20
Keck, J., Carrier, G. 1965. *J. Chem. Phys.* 43:2284–98
Kieffer, J. H., Lutz, R. W. 1966. *J. Chem. Phys.* 44:668–72
Knacke, R. F., Young, E. T. 1981. *Ap. J. Lett.* 249:L65–69
Knapp, G. R., Phillips, T. G., Huggins, P. J., Redman, R. D. 1981. *Ap. J.* 250:175–85
Kuiper, T. B. H., Zuckerman, B., Rodríguez-Kuiper, E. N. 1981. *Ap. J.* 251:88–102
Kwan, J. 1977. *Ap. J.* 216:713–23
Kwan, J., Scoville, N. 1976. *Ap. J. Lett.* 210:L39–44
Lepp, S., McCray, R. 1982. *Ap. J.* To be submitted
Levine, R. D., Bernstein, R. B., Kahana, P., Procaccia, I., Upchurch, E. T. 1976. *J. Chem. Phys.* 64:796–807
Levshakov, S. A., Varshalovich, D. A. 1979. *Ap. Lett.* 20:67–73
London, R. 1978. *Ap. J.* 225:405–16
London, R., McCray, R., Chu, S-I. 1977. *Ap. J.* 217:442–47
McGuire, P., Krüger, H. 1975. *J. Chem. Phys.* 63:1090–94
Morton, D. C., Dinerstein, H. L. 1976. *Ap. J.* 204:1–11

Mufson, S., Lyon, J., Marionni, P. A. 1975. *Ap. J. Lett.* 201:L85–89
Mullan, D. J. 1971. *MNRAS* 153:145–70
Nadeau, D., Geballe, T. R. 1979. *Ap. J. Lett.* 230:L169–74
Nadeau, D., Geballe, T. R., Neugebauer, G. 1982. *Ap. J.* 253:154–66
Nishimura, S. 1968. *Ann. Tokyo Astr. Obs.*, 2d ser. 11:33
Norman, C., Silk, J. 1978. *Ap. J.* 228:197–205
Norman, C., Silk, J. 1980. *Ap. J.* 238:158–74
Peebles, P. J. E., Dicke, R. H. 1967. *Ap. J.* 154:891–908
Persson, S. E., Geballe, T. R., Simon, T., Lonsdale, C. J., Baas, F. 1982. *Ap. J. Lett.* 251:L85–89
Radhakrishnan, V., Murray, J. D., Lockhart, P., Whittle, R. P. J. 1972. *Ap. J. Suppl.* 24:15–47
Rogerson, J. B., Spitzer, L., Drake, J. F., Dressler, K., Jenkins, E. B., Morton, D. C., York, D. G. 1973. *Ap. J. Lett.* 181:L97–102
Sargent, W. L. W., Young, P. J., Boksenberg, A., Tytler, D. 1980. *Ap. J. Suppl.* 42:41–81
Saslaw, W. C., Zipoy, D. 1967. *Nature* 216:976
Savage, B. D., Bohlin, R. C., Drake, J. F., Budich, W. 1977. *Ap. J.* 216:291–307
Schatz, G. 1976. PhD thesis. Calif. Inst. Technol.
Schatz, G., Kuppermann, A. 1976. *J. Chem. Phys.* 65:4668–92
Schwartz, R. D., Dopita, M. A. 1980. *Ap. J.* 236:543–48
Schwartz, R. N., Slawsky, Z. I., Herzfeld, K. F. 1952. *J. Chem. Phys.* 20:1591–99
Scoville, N. Z., Gezari, D. Y., Chin, G., Joyce, R. R. 1979. *Astron. J.* 84:1571–73
Scoville, N. Z., Hall, D. N. B., Kleinmann, S. G., Ridgway, S. T. 1982. *Ap. J.* 253: 136–48
Shull, J. M. 1978a. *Ap. J.* 219:877–85
Shull, J. M. 1978b. *Ap. J.* 224:841–47
Shull, J. M. 1980a. *Ap. J.* 234:761–64
Shull, J. M. 1980b. *Ap. J.* 237:769–80
Shull, J. M. 1982. In *Regions of Recent Star Formation: Proc. Symp. Neutral Clouds Near H II Regions*, ed. R. S. Roger, P. E. Dewdney, pp. 91–105. Dordrecht: Reidel. 496 pp.
Shull, J. M., Hollenbach, D. J. 1978. *Ap. J.* 219:877–85
Shull, J. M., York, D. G. 1977. *Ap. J.* 211:803–24
Simon, M., Righini-Cohen, G., Joyce, R. R., Simon, T. 1979. *Ap. J. Lett.* 230:L175–78
Smith, H. A., Larson, H. P., Fink, U. 1981. *Ap. J.* 244:835–43
Smoluchowski, R. 1981. *Astrophys. Space Sci.* 75:353–63
Snow, T. P. 1977. *Ap. J.* 216:724–37
Spitzer, L. 1976. *Q. J. R. Astron. Soc.* 17:97–120
Spitzer, L. 1978. *Physical Processes in the Interstellar Medium,* pp. 139–48. New York: Wiley-Interscience. 318 pp.
Spitzer, L., Cochran, W. D. 1973. *Ap. J. Lett.* 186:L23–28
Spitzer, L., Cochran, W. D., Hirshfeld, A. 1974. *Ap. J. Suppl.* 28:373–89
Spitzer, L., Jenkins, E. B. 1975. *Ann. Rev. Astron. Astrophys.* 13:133–64
Spitzer, L., Morton, W. A. 1976. *Ap. J.* 204:731–49
Spitzer, L., Zweibel, E. G. 1974. *Ap. J. Lett.* 191:L127–30
Stecher, T. P., Williams, D. A. 1967. *Ap. J. Lett.* 149:L29–30
Stokes, G. M. 1978. *Ap. J. Suppl.* 36:115–41
Strömgren, B. 1939. *Ap. J.* 89:526–47
Thompson, R. I., Lebofsky, M. J., Rieke, G. H. 1978. *Ap. J. Lett.* 222:L49–54
Thronson, H. A., Jr. 1981. *Ap. J.* 248:984–91
Treffers, R. R. 1979. *Ap. J. Lett.* 233:L17–20
Treffers, R. R., Fink, U., Larson, H. P., Gautier, T. N. 1976. *Ap. J.* 209:793–99
Turner, J., Kirby-Docken, K., Dalgarno, A. 1977. *Ap. J. Suppl.* 35:281–92
Watson, W. D. 1976. *Rev. Mod. Phys.* 48:513–52
Werner, M., Harwit, M. 1968. *Ap. J.* 154:881–89
Weymann, R. J., Carswell, R. F., Smith, M. G. 1981. *Ann. Rev. Astron. Astrophys.* 19:41–76
Wheeler, J. C., Mazurek. T. J., Sivaramakrishnan, A. 1980. *Ap. J.* 237:781–92
Wilson, R. W., Jefferts, K. P., Penzias, A. A. 1970. *Ap. J. Lett.* 161:L43–44
Wingert, D. W. 1975. *Ap. J.* 198:267–79
Yoneyama, T. 1972. *Publ. Astr. Soc. Jpn.* 24:87
Zarur, G., Rabitz, H. 1974. *J. Chem. Phys.* 60:2057–78
Zuckerman, B., Kuiper, T. B. H., Rodriguez-Kuiper, E. N. 1976. *Ap. J. Lett.* 209:L137–42